Chemical Reactivity of Lithium Doped Monolayer and Bilayer Graphene

1 AUTHOR:

Pablo A. Denis
University of the Republic, Uruguay

104 PUBLICATIONS **1,560** CITATIONS

# Chemical Reactivity of Lithium Doped Monolayer and Bilayer Graphene

Pablo A. Denis*,†,‡

†Computational Nanotechnology, DETEMA, Facultad de Química, UDELAR, CC 1157, 11800 Montevideo, Uruguay

‡Centro Interdisciplinario en Nanotecnología y Química Física de Materiales, Espacios Intersiciplinarios, UDELAR, Montevideo, Uruguay

ABSTRACT: Herein, we perform a comparative investigation on the reactivity of pristine and lithium doped monolayer and bilayer graphene. To study the addition of free radicals and 1,3 dipolar cycloadditions, we employed periodic DFT calculations. In all cases lithium increases the reactivity, even though the effect is weaker for the 1,3 dipolar cycloaddition as compared with that exhibited by free radicals. The effect of lithium doping is local and decreases as the functional group is attached far from the lithium atom. The increased reactivity can be explained by analyzing the band structure at the Fermi level. Lithium doped graphene is metallic thus showing an increased reactivity toward free radicals as observed for metallic nanotubes. However, the metallic character of lithium doped graphene is lost when free radicals like OH, SH, H, F, and CH_3 are attached; the Fermi level is raised and a gap is opened. The reactivity of bilayer graphene was almost unaffected by the lithium doping. Therefore, to enhance the reactivity of graphene it is crucial to use the monolayer form. Also, it is important to eliminate defects to decrease lithium diffusion to the other side of the sheet because Li atoms can remove the functional groups attached to graphene, forming compounds like LiOH, LiF, etc. Finally, for comparative purposes, we performed M06-2X and MP2 calculations for the addition of free radicals to lithium doped benzene. The results showed similar trends to those observed for graphene. This work demonstrates that lithium doping can dramatically increase the reactivity of graphene to such an extent that chemical groups that do not react with graphene become bonded when lithium is underneath. Thus, lithium doping can open new avenues for investigating the chemistry of the rather unreactive sp^2 framework of graphene.
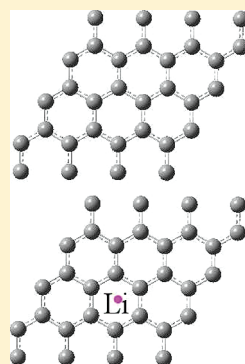
1. INTRODUCTION

Chemical functionalization of graphene is a powerful method to improve its chemical and physical properties. In particular, the modification of the covalent bonds in graphene can induce significant changes in its electronic structure. This effect can be attained by chemical functionalization[1−12] or by introducing heteroatoms in the framework of graphene.[13−20] As early as 2009 Bekyarova et al.[1] reported that the chemical modification of epitaxial graphene with aryl groups can open a band gap. The following year Elias et al.[2] showed that hydrogenation of graphene turns this material into an insulator. Yet, theoretical works showed that at high levels of hydrogenation graphene can be metallic.[6] In the same vein, the addition of nitrene radicals (NH) to graphene has been investigated. While it has been shown that graphene remains semimetallic even when one NH group is attached per 32 carbon atoms,[7] a band gap is opened if perfluorophenyazide is attached.[8] Upon variation of the number of NH groups, up to 100% of coverage band gaps as large as 4 eV can emerge. Regarding the organic chemistry of graphene, the most successful reaction is the 1,3 dipolar cycloaddition of azomethine ylides.[9−12] Although the theoretical works showed that this reaction can be attained only at defect sites or edges,[9,10] the experimental investigations indicated that this group can be grafted onto graphene by heating to 200−300 °C.[11,12] Despite

the modification of graphene structure by the addition of the azomethine group, we have found that at some concentrations the sheet remains semimetallic.[9] These results indicate that in some cases it is possible to tune the electronic structure of graphene by varying the functional groups that are covalently bonded to the sheet. However, there is an important problem to overcome in order to achieve that type of control. The perfect planar sp^2 framework of graphene lacks the curvature present in nanotubes and renders the sheet quite unreactive. For example, the addition energies of OH[4,5] groups to graphene are less than 12 kcal/mol and free radicals like SH[6] cannot be bonded to graphene. Therefore, it is important to find new approaches that can increase the reactivity of graphene. Recent experimental works by Billups group showed that lithium ammonia can disperse and increase the reactivity of nanotubes.[22,23] In the same line, Mandeltort et al.[24] analyzed the interaction between lithium doped nanotubes and chloromethane. They reported experimental and theoretical evidence which indicated that lithium not only increases the adsorption of chloromethane (CH_3Cl) but also catalyzes the C−Cl bond rupture in

chloromethane. The methyl (CH_3) radical is stabilized by a lithium atom and then it becomes chemically bound to defect sites of single wall carbon nanotubes (SWCNT), yielding alkylated nanotubes. The effect of lithium doping is not limited only to the covalent chemistry of SWCNTs. In effect, Buttner et al.[25] showed that doping SWCNTs with alkali metals increases the adsorption energies of nonpolar molecules, like n-heptane. Also, Jalbout showed that lithium increases the adsorption energies of amino acids onto fullerene (C_{60}).[26] The interest in lithium doped (Li-doped) nanostructures goes beyond the dispersing capabilities of lithium ammonia or the enhanced reactivity. Indeed, much work has been dedicated to shed light into the application of these doped nanostructures in the construction of anode materials[27,28] as well as to the crucial problem of hydrogen storage.[29,30] While the fundamental properties of Li-doped nanotubes[29−31] and fullerenes[26,32] have been investigated in extreme detail, the same is not true for the effect of lithium doping on chemical reactivity. The experimental results indicate that lithium doping enhances the reactivity of carbon nanotubes[21−24] and the adsorption of molecules onto nanotubes[26] and fullerenes.[26] However, for graphene, the information about the effect of lithium on its chemical reactivity is scarce. For these reasons, theoretical investigations on the reactivity of Li-doped graphene are certainly in need. In this work, we investigated two of the most common types of reactions entailing Li-doped monolayer and bilayer graphene: (a) the addition of free radicals, namely, hydroxyl (OH), thiol (SH), fluorine (F), CH_3, and hydrogen (H) and (b) the 1,3 dipolar cycloaddition of azomethine ylides. Theoretical calculations were carried out aiming to answer the following questions: (i) how is the reactivity of graphene affected by Li-doping; (ii) what is the comparative behavior of monolayer and bilayer graphene; (iii) does the lithium dopant increases the reactivity of 1,3 dipolar cycloadditions; (iii) which is the electronic structure of Li-doped graphene with functional groups attached? We expect that the present work can answer these questions thus clarifying the effect of lithium doping and stimulating new experimental and theoretical investigations about Li-doped graphene.

2. METHODS

The methodology employed herein is the same as the one we applied to successfully study the chemistry of graphene,[4,5,7,9,14−16,33] nanotubes,[34−38] and fullerenes.[9,39] Briefly, we performed density functional theory (DFT) calculations employing the Perdew—Burke—Ernzerhof (PBE) functional[40] for all carbon nanostructures, except in the case of bilayer graphene, for which we used the local density approximation (LDA)[41] method since PBE erroneously indicated a repulsive interaction between both layers. All periodic calculations were carried out with SIESTA,[42,43] which performs self-consistent field (SCF) calculations using numerical basis sets. For the latter we have selected the double-ζ basis set with polarization functions and fixed the orbital confining cutoff to 0.01 Ry. The split norm used was 0.15. The DFT implementation in SIESTA can be prone to significant basis set superposition error (BSSE), even with relatively low degree of radial confinement.[5] To avoid this problem, we used the counterpoise correction suggested by Boys and Bernardi.[44] In all cases, we employed relaxed structures to estimate the BSSE corrected binding energies and we took monomer deformation energies into account. The interaction between ionic cores and valence electrons was described by the Troullier—Martins norm

conserving pseudopotentials.[45] We have checked the convergence of the Mesh cutoff; using a value of 200 Ry, we obtained converged binding energies (within 0.02 eV). It is important to note that in our previous studies we performed methodology calibration against mesh cutoff and orbital confining cutoff values. By doing so, we were able to reproduce the results obtained without the use of pseudopotentials. Geometry optimizations were performed using the conjugate gradient algorithm until all residual forces were smaller than 0.01 eV/Å. To simulate infinite graphene sheets we used 4 × 4 and 5 × 5 supercells having 32 and 50 atoms, respectively, whereas for bilayer graphene we used two AB stacked 4 × 4 layers. We optimized the unit cells along the a and b directions and the c parameter was large enough to prevent interaction between adjacent sheets (25 Å). The unit cells were sampled using a 30 × 30 × 1 Monkhorst—Pack sampling, around 1000 k-points, similar to the one employed in our previous work about the chemical and electronic properties of doped graphene.[4,5,7,9,14−16,33]

In order to test the suitability of the PBE functional for the purposes of this work, we studied the reactivity of the benzene—lithium complex. This small system allows us to use more accurate methodologies, namely, M06-2X,[46] and Moller—Plesset second-order perturbation theory, MP2, method as implemented in Gaussian 2009.[47] The M06-2X functional is more accurate than the PBE[40] and LDA.[41] On the other hand, MP2 is expected to be free of the self-interaction error that accompanies inexact density functionals and thus it will provide an ab initio point of view. The basis sets employed for the benzene—lithium complex were the correlation consistent developed by Dunning and co-workers.[48]

3. RESULTS AND DISCUSSION

3.1. Reactivity of the Lithium—Benzene Complex. Prior to the investigation of the effect of lithium doping on the chemical reactivity of graphene, it is important to assess the performance of the PBE functional when studying the reactivity of lithium modified carbon based compounds. The system selected for such comparison was lithium doped benzene. We dubbed the increased reactivity of the Li-doped benzene as the "extra reactivity". It was calculated as the difference between the binding energy determined for the functionalized lithium doped benzene and those computed for the separated systems, i.e., when only one of them is attached to benzene. For example, at the M06-2X level the total binding energy of the Li and OH functional groups in the system Li—benzene + OH is 88.0 kcal/mol, whereas the binding energy for the attachment of OH to benzene is 19.9 kcal/mol. If we add the latter value to the complexation energy between Li and benzene (9.9 kcal/mol), we obtain a value of 29.8 kcal/mol for the sum of the OH and Li binding energies to benzene. The extra binding energy due to lithium doping is computed as 88.0 − 29.8 = 58.2 kcal/mol.

In Table 1 we list the extra binding energies computed for the five free radicals considered, and in Figure 1 we show the representative structures of the benzene + X and Li—benzene + X complexes. In all cases lithium increases the reactivity of benzene. Perhaps the most interesting case is portrayed by the SH group which cannot be bonded to benzene. Yet, when lithium is present on the other side of benzene, the binding energy is increased by 50 kcal/mol. The effect is stronger for fluorine, probably due to its large electronegativity, even though for OH it is only 3.7 kcal/mol weaker. Despite the increased reactivity of

Table 1. Electronic Binding Energies (kcal/mol) Determined at the M06-2X/cc-pVTZ Level for the Addition of Radicals to Bare and Lithium Doped Benzene

	total binding energy	extra binding energy	dist C$-$X (Å)
benzene$-$Li	9.9		2.205/2.112
benzene + F	34.7		1.407
benzene + OH	19.9		1.433
benzene + CH$_3$	13.4		1.544
benzene + SH	−3.93		1.898
benzene + H	24.8		1.100
Li$-$benzene + F	106.5	61.9	1.439
Li$-$benzene + OH	88.0	58.2[a]	1.441
Li$-$benzene + CH$_3$	73.9	50.6	1.533
Li$-$benzene + SH	55.9	50.0	1.912
Li$-$benzene + H	82.9	48.3	1.103

[a] Computed as 88.0 − 9.9 − 19.9.
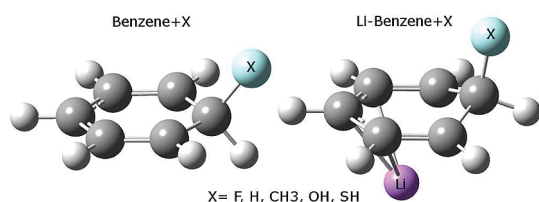
Figure 1. Optimized structures for bare and lithium doped benzene with different functional groups.

Table 2. Electronic Binding Energies (kcal/mol) Determined at Different Levels for the Addition of OH Bare and Lithium Doped Benzene

	total binding energy	extra binding energy	benzene$-$Li complexation energy	benzene + OH binding energy
M06-2X/cc-pVTZ	88.0	58.2	9.9	19.9
M06-2X/cc-pVQZ	88.6	58.3	10.3	20.0
PBE/cc-pVTZ	79.8	55.2	2.9	21.8
PBE/cc-pVQZ	85.7	52.9	8.8	23.0
PBE/DZP[a]	70.2	48.9	2.9	18.4
MP2/cc-pVTZ	84.7	79.9	1.0	3.8
MP2/cc-pVQZ	86.7	79.9	2.0	4.8

[a] Performed with SIESTA.

Table 3. Electronic Binding Energies (PBE/DZP, kcal/mol) for the Addition of Radicals and Azomethine to Bare and Lithium Doped Monolayer and Bilayer Graphene

	total binding energy	extra binding energy	dist C$-$X (Å)	gap (eV)
graphene 4 × 4 + Li	20.5			metal
graphene 5 × 5 + Li	22.6			metal
graphene 5 × 5 + F	34.1		1.502	metal
graphene 5 × 5 + OH	12.2		1.491	metal
graphene 5 × 5 + SH	0.0		2.949	metal
graphene 5 × 5 + CH$_3$	7.6		1.583	0.60
graphene 5 × 5 + H	21.4		1.137	0.65
graphene 5 × 5 + azomethine	15.9		1.600	semimetal
Li$-$graphene 5 × 5 + F	80.2	23.5	1.506	0.24
Li$-$graphene 5 × 5 + OH	58.1	23.3	1.482	0.28
Li-Graphene 5 × 5 + SH	40.4	17.8	1.995	0.31
Li$-$graphene 5 × 5 + CH$_3$	45.5	15.3	1.565	0.40
Li$-$graphene 5 × 5 + H	57.6	13.6	1.136	0.40
Li$-$graphene 5 × 5 + azomethine	44.5	6.0	1.586	metal

lithium doped benzene, the bond distances between the lithium−benzene complex and the functional groups are not increased but elongated, except in the case of the CH$_3$ radical. For the hydroxyl group the C−OH bond distance is 0.011 Å longer in the system with lithium. We consider that this behavior is due to an excess of electronic density located over benzene caused by lithium doping. Finally, we note that the formation of compounds like LiOH, LiF is thermodynamically preferred. However, we are not interested in those cases because the purpose of this work is to study the reactivity of lithium doped graphene. Therefore, if graphene has a small number of defects, migration of lithium will not be possible and it will remain unreactive underneath.

In recent work, Baker and Gordon used several DFT and ab initio methodologies to study the benzene−lithium complex. As explained by these authors even the most recent DFT methodologies are affected by the self-interaction error, which can induce erroneous results. For this reason, in Table 2 we include the extra binding energies computed for the Li−benzene + OH system obtained at the MP2 and DFT levels with different basis sets. Although there is a large variation in the binding energies computed with different methods, the MP2 results confirm the huge extra reactivity observed at the M06-2X level. Furthermore, MP2 predicts a much larger increased reactivity due to lithium doping. Therefore, we have confirmed that the additional reactivity due to lithium is not an artifact of the DFT methods. The results obtained at the PBE/cc-pVTZ and PBE/c-pVQZ levels are slightly smaller than those computed with M06-2X but they also indicate a significantly enhanced reactivity. Finally,

using the PBE implementation in SIESTA, we observe the same effect. Thus, we can be confident of the methodology selected for the periodic calculations carried out for graphene.

3.2. Reactivity of Lithium Doped Monolayer and Bilayer Graphene. We investigated the addition of F, OH, SH, CH$_3$, and H radicals as well as azomethine ylides to monolayer graphene. The addition energies and extra binding energies are presented in Table 3. Figure 2 shows the optimized structures for lithium doped graphene with and without functional groups. For the free radicals, the lithium atom is located in the hexagon that is bearing the radical. However, in the case of the 1,3 cycloaddition, the lithium atom is located below the CC bond where the reaction takes place. In contrast with the results obtained for benzene, we observe that for lithium doped graphene the distances between graphene and the free radicals are always shorter than those observed for pristine graphene. The sole exception is the fluorine for which the C−F bond distance is 0.003 Å longer. For the SH radical we observe the largest contraction of the C−X bond distance. In effect, it is reduced from 2.949 to 1.995 Å. Although the latter value is quite large
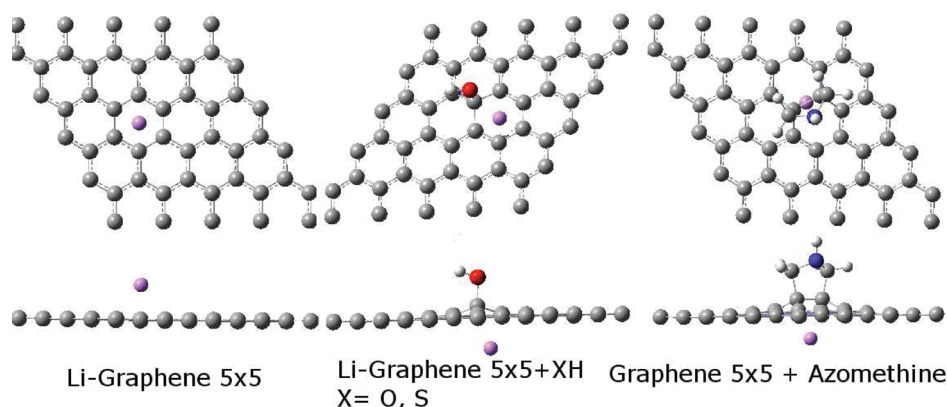
Figure 2. Optimized structures for lithium doped graphene with and without functional groups.
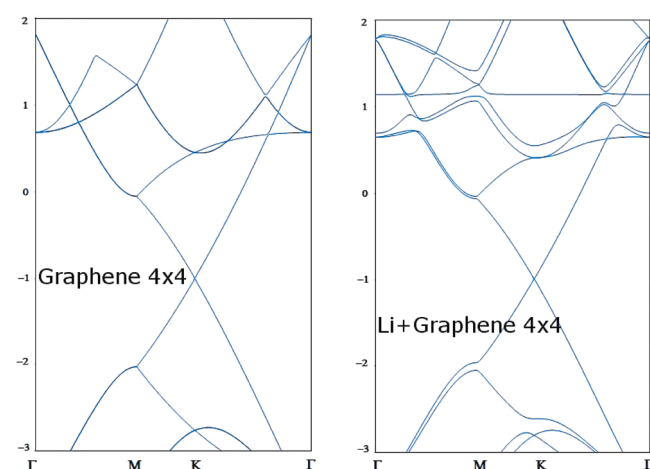

Figure 3. Band structure determined for pristine (left) and lithium doped bilayer graphene (right). The Fermi level is at 0 eV. (For the lithium doped graphene only the spin up band is shown, the spin down one is very similar.)
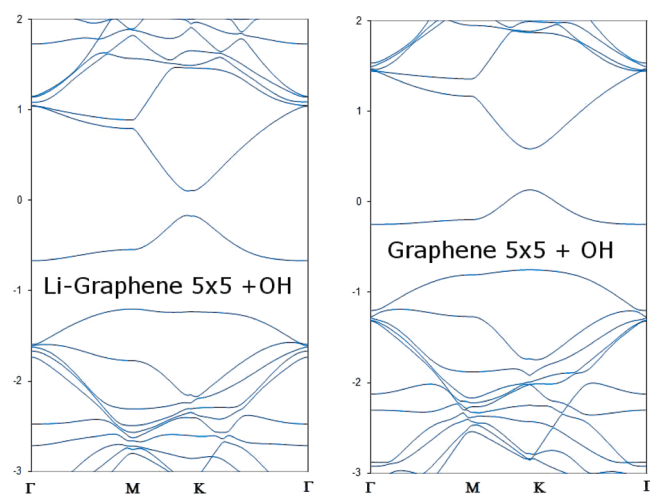

Figure 4. Band structure determined for pristine (right) and lithium doped bilayer graphene (left) functionalized with an OH radical. The Fermi level is at 0 eV.

for a C—S bond, the nature of the C—SH interaction is significantly changed by lithium doping.

Table 4. Electronic Binding Energies (kcal/mol) for the Addition of Hydrogen to Bare and Lithium Doped Monolayer and Bilayer Graphene

	total binding energy	extra binding energy	dist C−X (Å)
graphene 4 × 4−Li	29.8		
bilayer 4 × 4−Li	32.1		
graphene 4 × 4 + H	27.2		1.143
bilayer 4 × 4 + H over hexagon	28.4		1.142
bilayer 4 × 4 + H over carbon	27.4		1.138
graphene 4 × 4−Li + H	74.0	17.0	1.138
bilayer 4 × 4−Li + H over hexagon	63.3	2.8	1.139
bilayer 4 × 4−Li + H over carbon	61.6	2.1	1.142

In line with the results obtained for the benzene—lithium complex, lithium doping increases the reactivity of graphene. Yet, the effect is not that huge but nearly 50% smaller. The extra binding energies are 23.5, 23.3, 17.8, 15.3, 13.6, and 6.0 kcal/mol for the addition of F, OH, SH, CH_3, H, and azomethine ylides, respectively. The order of the extra binding energies computed for benzene is very similar to that observed in section 3.1. However, there are two small differences: for F and OH the effect is similar when graphene is considered and also the SH group exhibits a larger effect than the methyl radical. As mentioned in the previous paragraph, the thiol group is the most interesting case because it cannot be attached to pristine graphene but it reacts with lithium doped benzene. Hence, this result proves that lithium doping can open new avenues for investigating the chemistry of the rather unreactive sp^2 framework of graphene. It is important to note that if lithium is present in the same side as the functional groups, compounds like LiF, LiSH, and LiOH are formed. Therefore, to observe the increased reactivity due to lithium doping, it is mandatory to eliminate defects so as to decrease lithium diffusion to the other side of the sheet. Otherwise lithium will remove the functional groups covalently attached.

Next, we investigated whether the enhanced reactivity is a local effect or not. To this end we studied the addition of the CH_3 radical when the lithium atom is two hexagons away (6.2 Å from the addition site). The extra binding energy is 5.5 kcal/mol smaller as compared with that determined when lithium is below
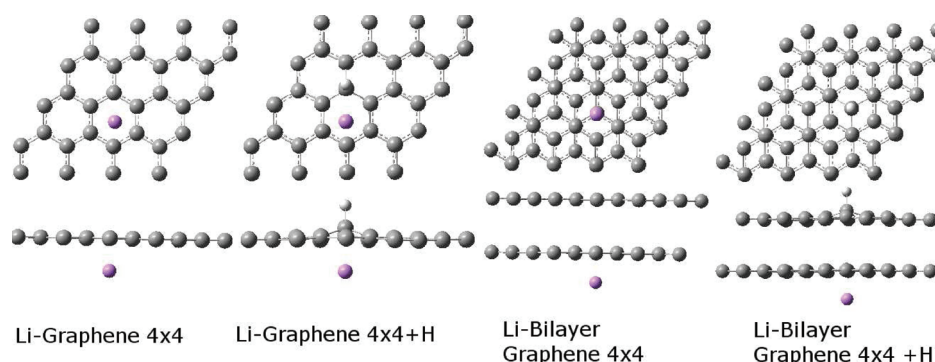
Li-Graphene 4x4   Li-Graphene 4x4+H   Li-Bilayer Graphene 4x4   Li-Bilayer Graphene 4x4 +H

Figure 5. Optimized structures for lithium doped monolayer and bilayer graphene with and without functional groups. For Li-doped bilayer graphene only the case with the hydrogen atom attached to a carbon atom that is over an hexagon is presented (the other case studied is when H is attached to a carbon that is over a carbon atom of the lowest layer).
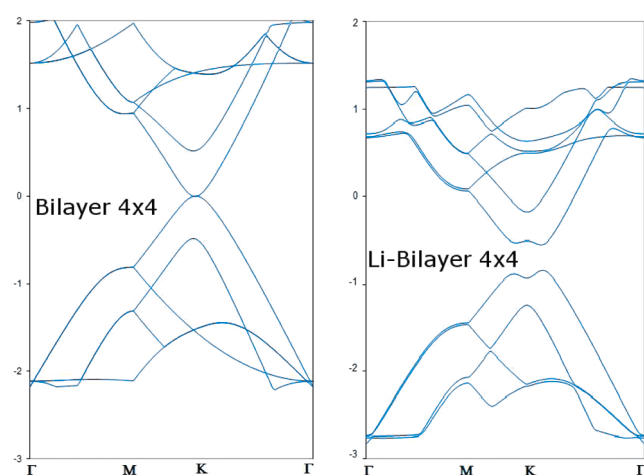

Figure 6. Band structure determined for pristine (left) and lithium doped bilayer graphene (right). The Fermi level is at 0 eV. (For the lithium doped bilayer graphene only the spin up band is shown, the spin down one is very similar.)

the hexagon bearing the methyl group. The analysis of the charge distribution supports that the effect is local. The charge transfer from lithium to graphene is 0.44 e$^-$. The charge donated to graphene is concentrated on the hexagon close to lithium. Indeed, 93% of the charge is shared by the six carbon atoms which are close to lithium. The band structure of bare and lithium doped graphene is presented in Figure 3. The lithium doping shifts the Fermi level to higher energies inducing a metallic character in the doped sheet. However, upon being functionalized the lithium doped graphene system suffers a metallic to semiconductor transition. In Figure 4 we show the band structure of one representative case, namely, the OH radical. When a free radical is attached to lithium doped graphene, a band gap is opened in the band structure of lithium doped benzene. Band gaps are listed in Table 3. They can be as large as 0.40 eV when the methyl radical is bonded to Li-doped graphene. The 1,3 dipolar cycloaddition has a different behavior. The addition of the azomethine ylide does not change the metallic character of lithium doped benzene.

The interaction between graphite and lithium has been extensively studied.[48,49] Valencia et al.[48] reported that the binding energy between lithium a graphite is 1.1 eV (25.4 kcal/mol) at the PBE level and using plane waves. The latter result is in good

agreement with our of 22.6 kcal/mol, which was obtained employing the less accurate but faster numerical basis sets based software. The charge transfer indicated by the Lowdin analysis was 0.6 e$^-$,[49] slightly larger than our Mulliken value. Nevertheless, employing the more sophisticated Bader analysis, the charge transfer was larger, 0.89 e$^-$ at the PBE level.[44] Recently, Baker and Head-Gordon[50] showed that DFT based methods may overestimate the amount of charge transfer between PAH and lithium because of the self-interaction error. We believe that in our case there is no artificial charge transfer because electron energy-loss spectroscopy showed that potassium transfers 0.7 e$^-$ to graphite[50] Therefore, bearing in mind the ionization potentials of lithium and potassium, a larger charge transfer is expected for lithium, in agreement with the Bader analysis performed by Valencia et al.[48] These pieces of evidence and the comparison performed in the previous section indicate that our methodology is adequate to investigate the effect of charge transfer on the reactivity of Li-doped graphene.

In the case of bilayer graphene, the comparison was performed using hydrogen. It is important to recall that the binding energies were computed at the LDA level because it works better than PBE in describing the interlayer interaction. The structures determined for lithium doped bilayer graphene are presented in Figure 5. For the addition of hydrogen, two sites were considered for bilayer graphene: (a) attachment of hydrogen onto a carbon atom located over a hexagon of the bottom layer; (b) attachment onto a carbon atom that is over one of the carbon atoms of the bottom layer. The C–H binding energies computed for both sites are very similar to the one determined for the monolayer, although the addition over a hexagon is 1.2 kcal/mol more stable. For monolayer graphene the extra binding energy is 17.0 kcal/mol at the LDA level. This value is 3.4 kcal/mol larger than the one determined with PBE. In the case of bilayer graphene we observe a small extra binding energy, 2.8 and 2.1 kcal/mol for cases a and b, respectively. This result is in agreement with the local effect of lithium doping. For bilayer graphene, the charge transferred from lithium is similar to that received by the monolayer and 87% of the charge is concentrated on the hexagon that is close to lithium. It follows that the amount of charge transfer to the upper layer (bonded to H) is almost nonexistent. The results obtained at the LDA level for bilayer graphene are supported by M06-L/3-21G calculations. Finally, in Figure 6 the band structure of bare and lithium doped bilayer graphene is depicted. The Fermi level is shifted toward higher

13396

dx.doi.org/10.1021/jp203547b |*J. Phys. Chem. C* 2011, 115, 13392–13398

energies, and in contrast with the results obtained for the monolayer, the degeneracy of the π and π^* bands at the K point is broken.

4. CONCLUSIONS

We have presented a comparative study of the effect of lithium doping on the addition of radicals and azomethine ylides to monolayer and bilayer graphene. The following are considered to be the most important findings of this work:

1. In all cases lithium increases the reactivity, even though the effect is weaker for the 1,3 dipolar cycloaddition as compared with free radicals. Similar trends were observed for the lithium—benzene complex.

2. The effect of lithium doping is local and decreases as the functional group is attached far from the lithium atom.

3. The reactivity of bilayer graphene is almost unaffected by lithium doping, whereas that of the monolayer was noticeably increased. It follows that for the lithium mediated enhancement of graphene activity it is crucial to obtain the monolayer form.

4. It is possible to induce a metallic to semiconductor transition for Li-doped graphene when free radicals are attached.

5. In order to observe the effect of lithium doping, it is important to eliminate defects to decrease lithium diffusion to the other side of the sheet because Li atoms can remove the functional groups attached to graphene, forming compounds like LiOH, LiF, etc.

6. Lithium doping makes possible the attachment of functional groups that cannot be added to bare graphene, as the attachment of SH to graphene.[26] Thus, lithium doping can open new avenues for investigating the chemistry of the rather unreactive sp^2 framework of graphene.

■ AUTHOR INFORMATION

Corresponding Author
*E-mail: pablod@fq.edu.uy.

■ REFERENCES

(1) Bekyarova, E.; Itkis, M. E.; Ramesh, P.; Berger, C.; Sprinkle, M.; de Heer, W. A.; Haddon, R. C. *J. Am. Chem. Soc.* **2009**, *131*, 1336.

(2) Elias, D. C.; Nair, R. R.; Mohiuddin, T. M. G.; Morozov, S. V.; Blake, P.; Halshall, M. P.; Ferrari, A. C.; Boukhvalov, D. W.; Katsnelson, M. I.; Geim, A. K.; Novoselov, K. S. *Science* **2009**, *323*, 610.

(3) Ghaderi, N.; Peressi, M. *J. Phys. Chem. C* **2010**, *114*, 21625.

(4) Denis, P. A.; Iribarne, F. *J. Mol. Struct.: THEOCHEM* **2009**, *907*, 93.

(5) Denis, P. A. *J. Phys.Chem. C* **2009**, *113*, 5612.

(6) Chandrachud, P.; Pujari, B. S.; Haldar, S.; Sanyal, B.; Kanhere, D. K. *J. Phys.: Condens. Matter* **2010**, *22*, 465502.

(7) Denis, P. A.; Iribarne, F. *J. Phys.Chem. C* **2011**, *115*, 195.

(8) Suggs, K.; Reuven, D.; Wang, X. -Q. *J. Phys. Chem. C* **2011**, *115*, 3313.

(9) Denis, P. A.; Iribarne, F. *Int. J. Quantum Chem.* **2010**, *110*, 1764.

(10) Cao, Y.; Houk, K. N. *J. Mater. Chem.* **2011**, *21*, 1503.

(11) Georgakilas, V.; Bourlnos, A. B.; Zboril, R.; Steriotis, T. A.; Dallas, P.; Stubos, A. K.; Trapalis, C. *Chem. Commun.* **2010**, 1766.

(12) Quintana, M.; Spyrous, K.; Grzelczak, M.; Browne, W. R.; Rudolf, P.; Prato, M. *ACS Nano* **2010**, *4*, 3527.

(13) Al-Aqtash, N.; Vasiliev, I. *J. Phys. Chem. C* **2009**, *113*, 12970.

(14) Denis, P. A.; Faccio, R.; Mombru, A. W. *ChemPhysChem* **2009**, *10*, 715.

(15) Denis, P. A. *Chem. Phys. Lett.* **2010**, *492*, 251.

(16) Denis, P. A. *Chem. Phys. Lett.* **2011**, *508*, 95.

(17) Dai, J.; Yuan, J.; Giannozzi, P. *Appl. Phys. Lett.* **2009**, *95*, 232105.

(18) Dai, J.; Yuan, J. *J. Phys.: Condens. Matter* **2010**, *22*, 225501.

(19) Ao, Z. M.; Yang, J.; Li, S.; Jiang, Q. *Chem. Phys. Lett.* **2008**, *461*, 276.

(20) Ao, Z. M.; Yang, J.; Li, S.; Jiang, Q. *Phys. Chem. Chem. Phys.* **2009**, *11*, 1683.

(21) Gong, S. J.; Sheng, W.; Chu, J. H. *J. Phys.: Condens. Matter* **2010**, *22*, 245502.

(22) Liang, F.; Sadana, A. K.; Chattopadhyay, J.; Gu, Z.; Hauge, R. H.; Billups, W. E. *Nano Lett.* **2004**, *4*, 1257.

(23) Chattopadhyay, J.; Chakraborty, S.; Mukherjee, A.; Wang, R.; Engel, P. S.; Billups, W. E. *J. Phys. Chem. C* **2007**, *111*, 17928.

(24) Mandeltort, L.; Buttner, M.; Yates, J. T.; Choudhury, P.; Xiao, L.; Johnson, J. K. *J. Phys. Chem. C* **2010**, *114*, 17148.

(25) Buttner, M.; Xiao, L.; Mandeltort, L.; Edington, S.; Johnson, J. K.; Yates, J. T. *J. Phys. Chem. C* **2009**, *113*, 4829.

(26) Jalbout, A. F. *J. Organomet. Chem.* **2008**, *693*, 1143.

(27) Li, J.; Wu, C.; Guan, L. *J. Phys. Chem. C* **2009**, *113*, 18431.

(28) Zhao, J.; Buldum, A.; Han, J.; Lu, J. P. *Phys. Rev. Lett.* **2000**, *85*, 1706.

(29) Liu, W.; Zhao, Y. H.; Li, Y.; Jiang, Q.; Lavernia, E. J. *J. Phys. Chem. C* **2009**, *113*, 2028.

(30) Liu, W.; Zhao, Y. H.; Li, Y.; Lavernia, E. J.; Jiang, Q. *Phys. Chem. Chem. Phys.* **2009**, *11*, 9233.

(31) Wen, Y. -W.; Liu, H. -J.; Jia, Y.; Pan, L.; Tan, X. J.; Shi, J. *Chin. Phys. Lett.* **2009**, *26*, 087102.

(32) Slanina, Z.; Uhlik, F.; Lee, S. -L.; Adamowicz, L.; Nagase, S. *Chem. Phys. Lett.* **2008**, *463*, 21.

(33) Denis, P. A.; Iribarne, F. *J. Mol. Struct.: THEOCHEM* **2010**, *957*, 114.

(34) Denis, P. A.; Faccio, R. *Chem. Phys. Lett.* **2008**, *460*, 486.

(35) Denis, P. A. *Int. J. Quantum Chem.* **2009**, *109*, 772.

(36) Denis, P. A.; Gancheff, J. S. *J. Mater. Sci.* **2010**, *45*, 1039.

(37) Denis, P. A.; Iribarne, F.; Faccio, R. *J. Chem. Phys.* **2009**, *130*, 194704.

(38) Denis, P. A. *Chem. Phys.* **2008**, *353*, 79.

(39) Denis, P. A.; Iribarne, F. *Int. J. Quantum Chem.* **2011**, DOI: 10.1002/qua.22940.

(40) Perdew, J. P.; Burke, K.; Ernzerhof, M. *Phys. Rev. Lett.* **1996**, *77*, 3865.

(41) Perdew, J. P.; Zunger, A. *Phys. Rev. B* **1981**, *23*, 5048.

(42) Soler, J. M.; Artacho, E.; Gale, J. D.; Garcia, A.; Junquera, J.; Ordejon, P.; Sanchez-Portal, D. *J. Phys.: Condens. Matter* **2002**, *14*, 2745.

(43) Ordejon, P.; Artacho, E.; Soler, J. M. *Phys. Rev. B* **1996**, *53*, R10441.

(44) Boys, F. S.; F. Bernardi, F. *Mol. Phys.* **1970**, *19*, 553.

(45) Troullier, N.; Martins, J. L. *Phys. Rev. B* **1991**, *43*, 1993.

(46) Zhao, Y.; Truhlar, D. G. *J. Chem. Phys.* **2006**, *125*, 194101.

(47) Frisch, M. J.; Trucks, G. W.; Schlegel, H. B.; Scuseria, G. E.; Robb, M. A.; Cheeseman, J. R.; Scalmani, G.; Barone, V.; Mennucci, B.; Petersson, G. A.; Nakatsuji, H.; Caricato, M.; Li, X.; Hratchian, H. P.; Izmaylov, A. F.; Bloino, J.; Zheng, G.; Sonnenberg, J. L.; Hada, M.; Ehara, M.; Toyota, K.; Fukuda, R.; Hasegawa, J.; Ishida, M.; Nakajima, T.; Honda, Y.; Kitao, O.; Nakai, H.; Vreven, T.; Montgomery, J. A., Jr.; Peralta, J. E.; Ogliaro, F.; Bearpark, M.; Heyd, J. J.; Brothers, E.; Kudin, K. N.; Staroverov, V. N.; Kobayashi, R.; Normand, J.; Raghavachari, K.; Rendell, A.; Burant, J. C.; Iyengar, S. S.; Tomasi, J.; Cossi, M.; Rega, N.; Millam, N. J.; Klene, M.; Knox, J. E.; Cross, J. B.; Bakken, V.; Adamo, C.; Jaramillo, J.; Gomperts, R.; Stratmann, R. E.; Yazyev, O.; Austin, A. J.; Cammi, R.; Pomelli, C.; Ochterski, J. W.; Martin, R. L.; Morokuma, K.; Zakrzewski, V. G.; Voth, G. A.; Salvador, P.; Dannenberg, J.J.; Dapprich, S.; Daniels, A. D.; Farkas, Ö.; Foresman, J. B.; Ortiz, J. V.; Cioslowski, J.;

13397

dx.doi.org/10.1021/jp203547b |*J. Phys. Chem. C* 2011, 115, 13392–13398

Fox, D. J. *Gaussian 09, Revision A.1*; Gaussian, Inc.: Wallingford, CT, 2009. Dunning, T. H., Jr. *J. Chem. Phys.* **1989**, *90*, 1007.

(48) Valencia, F. A.; Romero, A. H.; Ancilotto, F.; Silvestrelli, P. L. *J. Phys.Chem. B* **2006**, *110*, 14832.

(49) Li, Z. Y.; Hock, K. M.; Palmer, R. E.; Annett, J. F. *J. Phys.: Condens. Matter* **1991**, *3*, S103.

(50) Baker, T. A.; Head-Gordon, M. *J. Phys.Chem. A* **2010**, *114*, 10326.

13398

dx.doi.org/10.1021/jp203547b |*J. Phys. Chem. C* 2011, 115, 13392–13398